

Improved Transmission and Capture Data for Tantalum-181

J. M. Brown,^a G. Leinweber,^b D. P. Barry,^b B. Epping,^b M. Rapp,^b Y. Danon^a^aRensselaer Polytechnic Institute, 110 8th St, Troy, NY 12180, brownj25@rpi.edu^bNaval Nuclear Laboratory, P.O. Box 1072, Schenectady, NY 12301-1072

INTRODUCTION

As the nuclear energy community explores fast reactor concepts which utilize neutron populations more prevalent in the keV region, improved neutron cross section evaluation in this region is needed to make accurate models of such concepts. As neutron energy increases, resonances in the resolved resonance region (RRR) begin to overlap in energy space, causing some nuclear energy levels (resonances) to be missed during data collection and evaluation. As neutron energy is increased further, resonance overlap becomes more dominant and effectively averages the cross section in a region referred to as the unresolved resonance region (URR). The boundary between RRR and URR is not uniform among evaluations, resulting in differences in the cross section treatment, and therefore the evaluated cross section. These differences can in part be attributed to resonance self-shielding effects found in the way nuclear data is collected and stored.

MOTIVATION

Tantalum (Ta) is a prime example for highlighting differences in the RRR and URR treatments for the following reasons: it occurs naturally as a single isotope, meaning any given sample only needs to be chemically pure to avoid the complexity of contaminant resonances from other isotopes, nuclear data libraries ENDF/B-VII.1 and JEFF 3.2 have discrepant RRR and URR boundaries as well as discrepant URR cross section magnitudes, and it has been investigated for nuclear reactor applications [1, 2]. Differences in reaction rates resulting from such discrepancies can be demonstrated in applications such as the lead slowing down spectrometer (LSDS). As shown by Thompson [3], when using different nuclear data libraries to generate Ta cross section in MCNP simulations of the LSDS, the expected reaction rate no longer agrees beginning at the energy ENDF/B-VII.1 defined as the boundary between RRR and URR (330 eV). This is shown in Fig. 1 from Ref. 3. It can also be seen that the libraries that define the resolution boundary at a higher energy (2.4 keV) are capable of representing the fluctuations in cross section better than the combination of average cross section and probability tables used by MCNP to predict reaction rates in the URR.

These fluctuations in cross section become important, especially for calculating transmission of thick materials due to the increased effects of resonance self-shielding. As a

result, high resolution neutron transmission and capture yield data are needed to improve library cross sections. Along with high resolution measurements, there is a need for accurate error and covariance for ¹⁸¹Ta. These cross sections and associated covariance are important to accurately model any reactor system utilizing Ta.

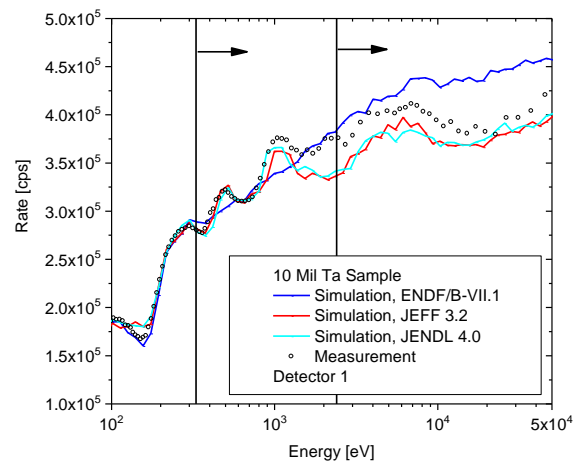


Fig. 1. Capture reaction rates for neutrons incident on Ta-181 recorded using a lead slowing down spectrometer. The first and second vertical lines and arrows represent the start of the URR for ENDF/B-VII.1 and JEFF-3.2/JENDL-4.0 respectively.

EXPERIMENTAL SETUP

The Gaertner Linear Accelerator Center at Rensselaer Polytechnic Institute (RPI) houses an electron linear accelerator (LINAC) which is often used to study nuclear data. The LINAC is operated by pulsing electrons and focusing klystron powered microwave radiation to accelerate pulsed electron packets towards a water-cooled Ta target at energies of ~55 MeV. Upon striking the target electrons interact with the atomic field of the Ta atoms and produce Bremsstrahlung radiation; the gammas produced by this reaction interact with the Ta nuclei in a (γ ,n) reaction producing a pulsed white source of neutrons. These neutrons are moderated by the water coolant and collimated by flight tubes kept under vacuum. Neutrons travel along the flight path, and are then recorded as having interacted with detectors at some distance from the target.

The time at which the (γ, n) reaction occurs and neutrons are produced is defined as t_0 , which is used to accurately measure the energies of neutrons produced in the target. The neutrons are all created at approximately the same time and place, but those with higher energy travel faster than those with lower energy, respectively corresponding to shorter and longer times in which they have traveled the same flight path. The equation used to describe the time energy relationship is similar to the description by the familiar kinetic energy equation. No relativistic corrections are required in this case because the neutrons being studied obtain much less energy than their rest mass. This relation is given by Eq. 1, where E_i is the energy of the neutron, t_i is the time at which a neutron interaction has been recorded, L is the flight path traveled, and k is a proportionality constant.

$$E_i = \left(\frac{k \cdot L}{t_i - t_0} \right)^2 \quad (1)$$

Ta samples were all 10x10 cm orthogonal to the LINAC beam, and approximately 1 mm (0.00566 at/b), 2 mm (0.01115 at/b), 3 mm (0.01713 at/b), and 6 mm (0.03358 at/b) thick along the path of the beam. Samples were ~99.9% chemically pure. Transmission was measured for sample thicknesses of 1, 3, and 6 mm and yield was measured for sample thicknesses of 1 and 2 mm. Transmission was also measured for a sample of depleted U with a thickness of 1.587 cm (0.0761 at/b) in order to verify experimental quantities with a well known sample.

The RPI LINAC was operated with a pulse width of ~8 ns and repetition rate of 400 Hz. Transmission was measured at ~100 m along the center beam path with the Mid-Energy Li-glass Neutron Detector Array (MELINDA) [4], which is described in detail in Ref. 4. Capture yield was measured at ~45 m along the east beam path using C_6D_6 detectors optically coupled to photomultiplier tubes. The transmission and capture systems recorded events with time bins of size 6.4 and 0.8 ns respectively.

ANALYSIS

For this experiment, two methods of detection were employed in an effort to measure both the total neutron interaction cross section and the neutron capture cross section. To measure the total cross section σ_t , the transmission T of ^{181}Ta was measured, which involves measuring the count rate in the LINAC beam with and without a sample between the target and detector and calculating the ratio of these count rates using Eq. 2. To measure the capture cross section σ_γ the relative neutron rate φ_{rel} in the LINAC beam is measured, and a sample is then placed in the beam to determine the capture rate. The ratio of capture rate and neutron rate is the yield Y .

$$\frac{\dot{C}_s - \dot{B}_s - \dot{B}_{0,s}}{\dot{C}_o - \dot{B}_o - \dot{B}_{0,o}} = T = e^{-N\sigma_t} \quad (2)$$

These can be related to experimental quantities by Eq. 2 and Eq. 3, where N is the sample thickness in [atoms/barn], \dot{C}_s is the count rate with a sample in the beam, \dot{C}_o is the open or sample out count rate, $B_{s,o}$ are the time dependent backgrounds made up of gammas and off energy neutrons, and $B_{0,s,o}$ are the time independent backgrounds measured at very large times of flight.

$$\frac{\dot{C}_\gamma - \dot{B}_\gamma}{\varphi_{rel}} = Y = \frac{\sigma_\gamma}{\sigma_t} (1 - e^{-N\sigma_t}) \quad (3)$$

The count rate with a sample in the beam is given by C_γ , and weighted according to the gamma detection efficiency corresponding to the sample/detector geometry and gamma energy deposition [5]. B_γ is the background made up of scattered in beam photons and naturally occurring gamma radiation determined by the proxy sample method [5] described in Ref. 5, φ_{rel} is determined from the capture rate of a well-known sample, in this case B_4C , which is described by Eq. 4.

$$\varphi_{rel} = \frac{\dot{C}_{B_4C} - \dot{B}_{B_4C}}{Y_{B_4C}} \quad (4)$$

The count rate from capture reactions with a B_4C sample in the LINAC beam is given by \dot{C}_{B_4C} , B_{B_4C} is the in-beam background associated with the B_4C measurement, and Y_{B_4C} is determined by MCNP 6.1 calculations of capture yield. The count rates for both transmission and capture were dead time corrected, and monitors (fission chambers) were used to normalize for and verify accelerator beam stability. From Eq. 3 it can be seen that knowledge of the total cross section is essential for accurate measurement of the capture cross section. With the combination of transmission and capture yield, the evaluation of the capture cross section is not reliant on previous measurements.

RESULTS

Experimental quantities such as the precise t_0 , flight path length L , or experimental resolution function can be verified by measuring a well-known material such as depleted U. Depleted U (1.587 cm) was an additional sample during the measurement, and transmission for the sample has been plotted in Fig. 2. As seen in Fig. 2 the depleted U sample transmission curve matches well with the SAMMY 8.0 calculated transmission, verifying experimental quantities previously mentioned as well as the calculated open

background count rate \dot{B}_0 which is used to calculate the final transmission.

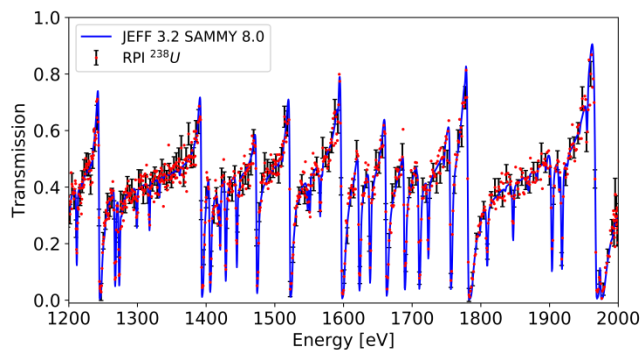


Fig. 2. Transmission of depleted U compared to the theoretical curve calculated by SAMMY 8.0 using resonance parameters obtained from JEFF 3.2.

Having constrained the experimental parameters with the dep. U, the transmission for the Ta samples can be produced and plotted along with the expected values given by JEFF 3.2 as shown in Fig. 3. All SAMMY 8.0 calculated curves are in blue and are calculated from JEFF 3.2 resonance parameters and include experimental quantities such as the experimental resolution function, sample thickness, and flight path length. The transmission of each thickness Ta sample was calculated using the same background procedure as the depleted U, as well as the same open beam count rate C_0 and corresponding background count rate \dot{B}_0 .

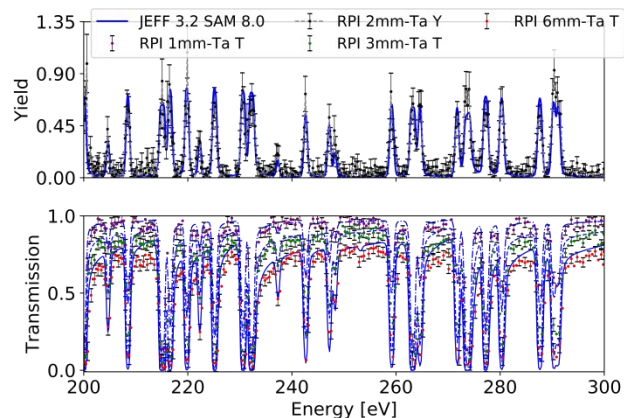


Fig. 3. Neutron capture yield for the 2 mm thick Ta sample (top), and neutron transmission for 1, 3, and 6 mm Ta samples.

This experiment focused on neutron energies from the RRR in ENDF/B-VII.1 (330 eV) to the end of URR in JEFF 3.2 (100 keV). The background procedure constrains the accurate measurement of the background to between ~0.150-80 keV. The lower energy transmission and yield are shown in Fig. 3, the energy region between JEFF 3.2

and ENDF/B-VII.1 resolution boundaries is shown in Fig. 4 where the blue curves represent SAMMY 8.0 calculations of transmission and yield based on JEFF 3.2 resonance parameters.

As seen in Fig. 4, much of the resonant structure in the ENDF/B-VII.1 URR can be represented by resonance parameters and used to calculate both yield and transmission. ENDF/B-VII.1 currently stores average resonance parameters and uses a probability table treatment to account for fluctuations in URR cross section when users wish to create ACE files. In future ENDF evaluations it may prove beneficial to extend the RRR to higher energies in order to preserve more information about the cross section and better represent calculations such as yield and transmission. This is important, for example, in the transmission through a thick sample where self-shielding becomes significant.

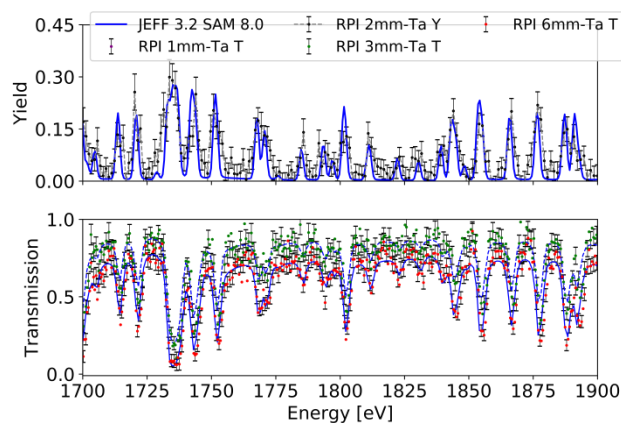


Fig. 4. Neutron capture yield for the 2mm thick Ta sample (top), neutron transmission for Ta samples 3 and 6 mm thick.

CONCLUSIONS

Neutron transmission and capture yield of ^{181}Ta were measured to generate more accurate resonance parameters and covariance data for those parameters. Incorporation of these data into an evaluation of Ta has the opportunity to improve the resulting cross sections and provide covariance information where there were none readily available. The combination of transmission and capture yield experimental data allow for a full evaluation of ^{181}Ta where experimental parameters such as beam energy, target material, repetition rate, and pulse width can be kept uniform for the experiment. This reduces inaccuracies due to the normalization of data and background subtraction from quantities of interest.

ACKNOWLEDGMENTS

The authors wish to thank the RPI technical staff: Peter Brand, Larry Krusieski, Azeddine Kerdoun, Michael Bretti, and Matt Gray for their operation of the LINAC and the enormous amount of technical expertise they offer.

REFERENCES

1. D. LOAIZA, D. GEHMAN, R. SANCHEZ, D. HAYES, and M. ZERKLE, "Critical mass and subcritical experiments interlaced with Nb-1Zr, Re, Mo, Ta-2.5W fuels with highly enriched uranium in support of the Prometheus project," *Nucl. Sci. Eng.*, **160**, no. 2, pp. 217-231 (2008).
2. R.L. KLUEH, A.T. NELSON, "Ferritic/Martensitic Steels for Next Generation Reactors," *Journal of Nuclear Materials*, **371**, pp. 37-52 (2007).
3. N. THOMPSON, "Measuring and Validating Neutron Cross Sections Using a Lead Slowing Down Spectrometer," Ph.D. Dissertation, Mech. Aero. Nucl. Eng. Dept., RPI (2017).
4. R. BAHRAN, "A New High Energy Neutron Transmission Detector at the Gaertner LINAC Center and Isotopic Molybdenum Total Cross Section Measurements in the keV-Region," Ph.D. Dissertation, Mech. Aero. Nucl. Eng. Dept., RPI (2013).
5. B. MCDERMOTT, "Resonance Region Capture Cross Section Measurements in Iron and Tantalum Using a New C_6D_6 Detector Array," Ph.D. Dissertation, Mech. Aero. Nucl. Eng. Dept., RPI (2016).